Structural Investigations of Sulfite-Bridged Binuclear Complexes of Platinum(II) and Palladium(II)

Roland Krieglstein,[a] Dietrich K. Breitinger,*[a] and Günther Liehr[a]

Keywords: Palladium / Platinum / O,S ligands / Structure elucidation / Vibrational spectroscopy

Although analogous platinum(II) and palladium(II) compounds usually show similar chemical behaviour, different reaction products have been obtained on reaction of ethane-1,2-diamine bissulfitometallates(II) with the diaqua ethane-1,2-diamine metal(II) complexes of Pt and Pd. – The crystal structures of bis(μ-sulfito-1κS:2κO)bis[(ethane-1,2-diamine)-platinum(II)] trihydrate $[(en)Pt(SO_2O)_2Pt(en)]\cdot 3\,H_2O$ (**1**) with parallel μ-(S:O) sulfite bridges, and of bis[(ethane-1,2-diamine)-μ-(S:O)-sulfitopalladium(II)] trihydrate $[(en)Pd(SO_2O)(OO_2S)Pd(en)]\cdot 3\,H_2O$ (**2**) with antiparallel bridges, have been determined by single-crystal X-ray structure analyses. In both compounds the complex units are held together mainly by a complicated network of hydrogen bonds including the hydrate water molecules. – In contrast to the complex molecules in **1** with parallel bridges, the complex units of **2** possess an inversion centre. As a result the mutual exclusion rule reduces the number of bands in each of the vibrational spectra of **2** to half that in the spectra of **1**. This effect is most clearly seen in the number of the valence vibrations $\nu(MN_2)$; the Raman spectrum of **1** displays four relatively strong bands, whereas the Raman spectrum of **2** shows only two, as expected. Further, features of the vibrational spectra are in agreement with the findings of the crystal and molecular structures. Thus, the *trans*-influence exerted by the *S*-coordinated sulfites onto the M–N bonds in the *trans*-position induces a significant lengthening and weakening of these bonds relative to the M–N bonds *trans* to oxygen. In the Raman spectrum of **1** the valence vibrations of the PtN_2 group *trans* to sulfur are clearly lowered in frequency.

Introduction

Our group has been involved with the syntheses, crystal structures, and vibrational spectra of the sulfito complexes of the platinum-group metals for some time. In these studies particular attention has been paid towards the effects of the *trans*-influence of the sulfite ligands.

It has been shown by X-ray structure analysis and vibrational spectroscopy that the anions in the compounds $K_2[M^*(SO_3)_2]$ (M* = Pd and Pt) are coordination polymers in which the metal atoms are connected by pairs of sulfite groups forming parallel μ-(S:O) bridges.[1,2]

After the preparation of a non-polymeric trinuclear cobalt complex with triple parallel μ-(S:O) bridges,[3] it seemed feasible to form related dinuclear sulfite-bridged complexes of the platinum-group metals involving the isolated repeat units in the above mentioned coordination polymers. A possible synthetic pathway would be the condensation of the cation *cis*-$[L_2M^*(OH_2)_2]^{2+}$ and the anion *cis*-$[L_2M^*(SO_3)_2]^{2-}$ to yield the neutral complex $[L_2M^*(SO_2O)_2M^*L_2]$. It was not possible to use a complex with $L = NH_3$ as a terminating ligand for this purpose (as in the case of the above cobalt complex), since it was previously found that the anion *cis*-$[Pd(SO_3)_2(NH_3)_2]^{2-}$ undergoes *cis*-*trans*-isomerisation in aqueous solution.[1a] Hence, the chelating ligand ethane-1,2-diamine (en), which prevents this rearrangement, was chosen as terminating ligand. The preparation of the complexes $[(en)M^*(OH_2)_2]^{2+}$ and $[(en)M^*(SO_3)_2]^{2-}$ are well-documented (see ref.[4]).

Based on limited IR[5] and Raman spectra,[6] the existence of a palladium complex with antiparallel double sulfite bridges has already been suggested.

Although analogous platinum and palladium compounds usually show similar chemical behaviour in their reactions of the aqua complexes $[(en)M^*(OH_2)_2]^{2+}$ with the disulfitometallates $[(en)M^*(SO_3)_2]^{2-}$, different final reaction products are obtained. For M* = Pt, the complex bis(μ-sulfito-1κS:2κO)bis[(ethane-1,2-diamine)platinum(II)] trihydrate $[(en)Pt(SO_2O)_2Pt(en)]\cdot 3\,H_2O$ (**1**) with parallel bridges is formed, and for M* = Pd, the species bis[(ethane-1,2-diamine)-μ-(S:O)-sulfitopalladium(II)] trihydrate $[(en)Pd(SO_2O)(OO_2S)Pd(en)]\cdot 3\,H_2O$ (**2**) with antiparallel bridges is formed (see Scheme 1).

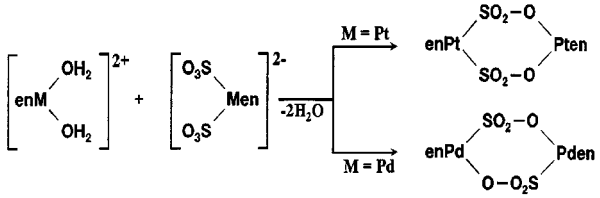

Scheme 1

Results and Discussion

Crystal Structure Analyses

Both complexes **1** and **2** could be obtained as single crystals by recrystallisation from aqueous media, under care-

[a] Institute of Inorganic Chemistry,
University of Erlangen-Nürnberg,
Egerlandstraße 1, 91058 Erlangen, Germany
Fax: (internat.) + 49-9131/85 27387
E-mail: Breitinger@chemie.uni-erlangen.de

  1434–1948/01/1212–3067 $ 17.50+.50/0

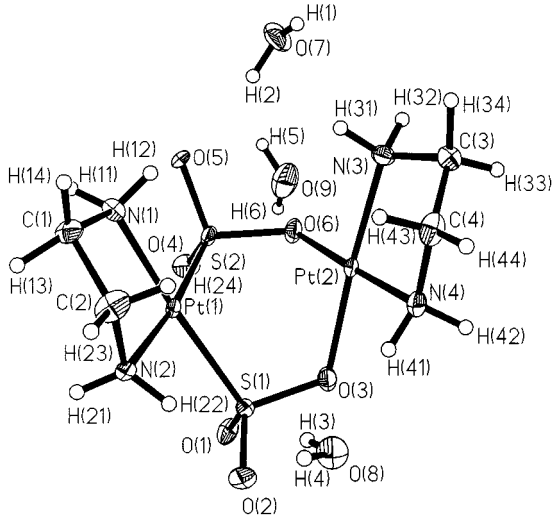

Figure 1. ORTEP plot of the dinuclear complex unit of **1**

fully controlled conditions (see Exp. Sect.). Table 4 lists the relevant crystallographic data.

Figure 1 shows the molecular structure of the dinuclear complex unit of **1**, including one set of the three independent water molecules.

Bond lengths and angles for both compounds are presented in Table 1 and Table 2.

All bond lengths and angles in the complex unit $[(en)Pt(SO_3)_2Pt(en)]$ of **1** (with no crystallographically imposed symmetry) are as expected. Thus, the chemically equivalent Pt−N bonds in each of the two different chelate rings, as well as the chemically equivalent Pt−S and Pt−O bonds are the same within their e.s.d's. However, the averaged Pt(1)−N bonds [$\bar{r}$ = 2.09(1) Å] are significantly longer than the Pt(2)−N bonds [$\bar{r}$ = 2.02(1) Å], clearly showing the differences in the *trans*-influence of sulfite when coordinated through sulfur and oxygen. Further, the angles N−Pt(1)−N [81.9(4)°] and N−Pt(2)−N [84.2(5)°] deviate substantially from 90°. This is also suggested by the sequences $\nu_s > \nu_{as}$ of the valence frequencies of the two PtN_2 entities in the Raman spectrum of **1**.[7]

The S(1)−O(3) and S(2)−O(6) bonds, which form part of the sulfite bridges in **1**, are clearly longer [$\bar{r}$ = 1.533(8) Å] relative to the four terminal S−O bonds [$\bar{r}$ = 1.468(9) Å], which do not deviate significantly from each other. This is similar to the findings in the structure of $K_2[Pd(SO_3)_2]\cdot H_2O$.[1b] The bonding data of these μ-(S:O) bridging sulfite ligands are similar to those in the less precisely determined structure of a dinuclear organometallic complex $[Pt_2(\mu\text{-}SO_3)(\mu\text{-}SO_2)(COD)_2]$ (COD = cycloocta-1,5-diene).[8]

Both μ-(S:O)-bridged platinum atoms display an approximately square-planar environment comprising pairs of nitrogen atoms *cis* to one another, and pairs of sulfur and oxygen atoms at Pt(1) and Pt(2), respectively. The five atoms in each of these groups deviate from the respective least-squares plane by a maximum of 0.099 Å for the $Pt(1)N_2S_2$ group, and by a maximum of 0.025 Å for the $Pt(2)N_2O_2$ group (see Table 3).

The central ring $Pt(1)(S-O)_2Pt(2)$ in **1** adopts a boat conformation in contrast to the chair conformation in **2**.

In **1** two molecules are arranged around an inversion centre such that their Pt(2) atoms are 3.0441(9) Å apart (Figure 2). This is a remarkably short distance. The conformations of the two en ligands within one molecule are different. However, due to the inversion centre between the two molecules, their symmetry-related en-rings adopt δ- and λ-conformations, respectively.

Table 1. Bond lengths and angles of **1**; e.s.d.'s are given in parentheses

Bond lengths [Å]		N(2)−Pt(1)−S(2)	172.8(3)
Pt(1)−N(1)	2.08(1)	N(3)−Pt(2)−N(4)	84.2(5)
Pt(1)−N(2)	2.10(1)	O(3)−Pt(2)−O(6)	88.9(4)
Pt(2)−N(3)	2.02(1)	N(3)−Pt(2)−O(3)	176.0(4)
Pt(2)−N(4)	2.01(1)	N(3)−Pt(2)−O(6)	94.3(4)
Pt(1)−S(1)	2.244(3)	N(4)−Pt(2)−O(3)	92.6(4)
Pt(1)−S(2)	2.243(3)	N(4)−Pt(2)−O(6)	178.1(4)
Pt(2)−O(3)	2.044(9)	Pt(1)−S(1)−O(1)	116.3(4)
Pt(2)−O(6)	2.070(9)	Pt(1)−S(1)−O(2)	110.9(4)
S(1)−O(1)	1.475(9)	Pt(1)−S(1)−O(3)	105.1(4)
S(1)−O(2)	1.471(9)	O(1)−S(1)−O(2)	109.9(6)
S(1)−O(3)	1.528(8)	O(1)−S(1)−O(3)	108.3(5)
S(2)−O(4)	1.461(9)	O(2)−S(1)−O(3)	105.6(5)
S(2)−O(5)	1.463(9)	Pt(1)−S(2)−O(4)	114.7(4)
S(2)−O(6)	1.537(8)	Pt(1)−S(2)−O(5)	108.0(4)
N(1)−C(1)	1.50(2)	Pt(1)−S(2)−O(6)	108.6(4)
N(2)−C(2)	1.49(2)	O(4)−S(2)−O(5)	111.3(6)
N(3)−C(3)	1.48(2)	O(4)−S(2)−O(6)	106.9(5)
N(4)−C(4)	1.48(2)	O(5)−S(2)−O(6)	107.2(5)
C(1)−C(2)	1.49(2)	S(1)−O(3)−Pt(2)	119.1(5)
C(3)−C(4)	1.48(2)	S(2)−O(6)−Pt(2)	113.8(5)
Pt(2)−Pt(2)[a]	3.0441(9)	Pt(1)−N(1)−C(1)	110.9(8)
Pt(1)−Pt(2)	3.1263(7)	C(2)−N(2)−Pt(1)	106.8(8)
Bond angles [°]		Pt(2)−N(3)−C(3)	108.7(8)
N(1)−Pt(1)−N(2)	81.9(4)	C(4)−N(4)−Pt(2)	108.3(8)
S(1)−Pt(1)−S(2)	92.8(1)	N(1)−C(1)−C(2)	111(1)
N(1)−Pt(1)−S(1)	171.7(3)	C(1)−C(2)−N(2)	108(1)
N(1)−Pt(1)−S(2)	91.1(3)	N(3)−C(3)−C(4)	108(1)
N(2)−Pt(1)−S(1)	94.4(3)	C(3)−C(4)−N(4)	108(1)

[a] $1-x, 2-y, 1-z$.

Table 2. Bond lengths and angles of **2**; e.s.d.'s are given in parentheses

Bond lengths [Å]		O(3)−Pd−N(2)	172.3(2)
Pd−N(1)	2.079(4)	O(3)−Pd−N(1)	90.6(1)
Pd−N(2)	2.019(4)	S−Pd−O(3)	93.5(1)
Pd−S	2.229(1)	Pd−S−O(1)	111.6(1)
Pd−O(3)	2.043(3)	Pd−S−O(2)	109.2(1)
S−O(1)	1.466(3)	Pd−S−O(3)[a]	110.1(1)
S−O(2)	1.479(3)	O(1)−S−O(2)	111.2(2)
S−O(3)[a]	1.501(3)	O(1)−S−O(3)[a]	105.5(2)
N(1)−C(1)	1.484(6)	O(2)−S−O(3)[a]	109.1(2)
N(2)−C(2)	1.492(6)	Pd−O(3)−S[2]	128.0(2)
C(1)−C(2)	1.493(7)	Pd−N(1)−C(1)	109.4(3)
Bond angles [°]		Pd−N(2)−C(2)	108.9(3)
N(2)−Pd−N(1)	82.8(2)	N(1)−C(1)−C(2)	106.9(4)
S−Pd−N(1)	175.8(1)	N(2)−C(2)−C(1)	108.3(4)
S−Pd−N(2)	93.1(1)		

[a] $1-x, 1-y, 1-z$.

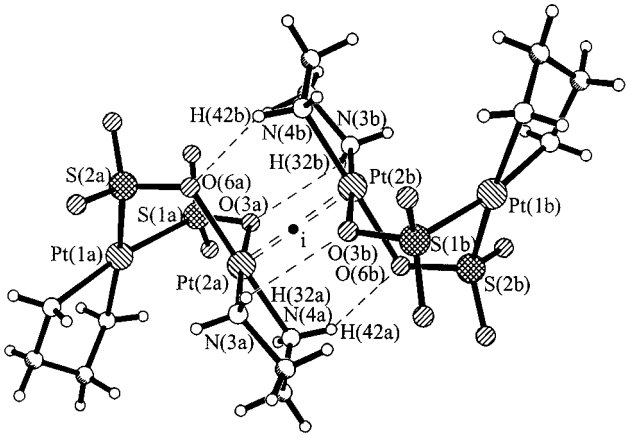

Figure 2. Arrangement of the complex units of **1** into dimers

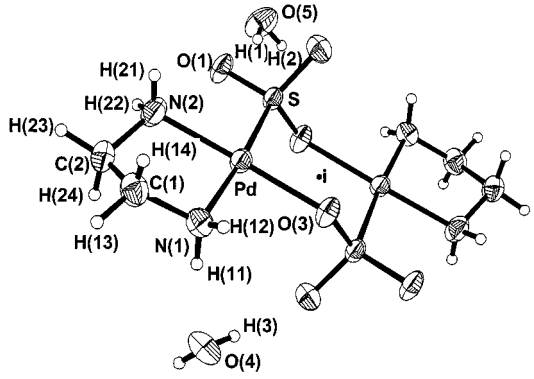

Figure 3. ORTEP plot of the dinuclear complex unit of **2**

Table 3. Deviation from the least-square planes through the metal atoms and their environments in **1** and **2**

$Pt(1)N_2S_2$ plane of **1**		$Pt(2)N_2O_2$ plane of **1**		PdN_2SO plane of **2**	
Pt(1)	−0.049(3)	Pt(2)	−0.025(4)	Pd	0.021(1)
N(1)	0.099(4)	N(3)	0.016(5)	N(1)	0.045(2)
N(2)	−0.072(4)	N(4)	−0.004(5)	N(2)	−0.053(2)
S(1)	0.083(4)	O(3)	0.016(5)	S	0.037(1)
S(2)	−0.061(4)	O(6)	−0.003(5)	O(3)	−0.050(2)

The above-mentioned short intermolecular Pt···Pt distance may suggest that metal-to-metal interactions could contribute to the cohesion of the molecules in the lattice. Square-planar complexes of d^8-metals that are stacked in columns or chains, with overlapping d_{z^2} orbitals, are well-known. Thus, chain-structured Krogmann salts (obtained by partial oxidation of $K_2[Pt(CN)_4]$) show Pt−Pt distances between 2.87 and 2.96 Å, in comparison with the distance of 2.78 Å in platinum metal.[9] In the structure of **1** there are no such chain-like arrangements, but only isolated pairs of close Pt atoms in antiparallel (inversion correlated) N_2PtO_2 groups. A situation similar to that in **1** is found in $[(NH_3)_2Pt(OH)_2Pt(NH_3)_2]CO_3{\cdot}2\,H_2O$, where an intermolecular metal-to-metal distance of 3.167(1) Å is found.[10] In this case, the authors precluded attractive interactions between the platinum atoms, since they deviate from the least-squares planes, containing the atoms coordinated to the Pt atoms, such that the Pt···Pt distance increases. Consequently, the cohesion within a pair of complex units is attributed to four hydrogen bonds N−H···O.

Similarly, in **1** the platinum atom Pt(2) is shifted from the least-squares plane through the ligand atoms N(3), N(4), O(3) and O(6) by 0.031(5) Å, such that the Pt···Pt distance increases again. Once more, four hydrogen−bonds, N−H···O, apparently hold the two molecules together. Although these individual hydrogen−bonds, with O···N distances of 2.98(1) and 2.99(1) Å, and unfavourable bond angles are considered to be weak, their cooperation effects the cohesion in these pairs of molecules.

Thus, a complex network of these hydrogen bonds, and of further hydrogen bonds involving the water molecules, hold the constituents of this crystal structure together.

The remarkably poor stability of the crystals in air under ambient conditions can be attributed to the fewer appropriate partners available for hydrogen bonding with the lattice water molecule $H_2O(9)$. Further, one of the two hydrogen bonds [N(4)···O(9)] with a distance of 2.96(1) Å is weak. These facts are in accordance with the findings of the TGA/DTA analysis of the substance. They show that the loss of just one water molecule per formula unit occurs at a temperature as low as 30 °C; the further loss of two lattice water molecules occurs by about 140 °C.

The molecular structure of **2** is shown in Figure 3. The respective bond lengths and angles are presented in Table 2.

The two palladium centres in **2** are μ-(S:O) bridged by two sulfite groups in an antiparallel arrangement. The coordination around these equivalent Pd atoms is square-planar, with two non-equivalent nitrogen atoms *cis* to one another, one oxygen atom and one sulfur atom. The five atoms deviate from the ideal plane by a maximum of 0.05 Å (see Table 3). The $(Pd-S-O)_2$ ring adopts a chair conformation, in contrast to the central ring in the platinum compound **1** (see above). Since the molecules in **2** are centrosymmetric, their equivalent Pd(en) rings adopt opposite δ- and λ-conformations, respectively. While the oxygen atom O(4) of one lattice water molecule is located on a C_2-axis (Wyckoff 4e), the second water molecule and all the other atoms are distributed on general sites (Wyckoff 8f).

The Pd−N(2) bond [2.019(4) Å] is significantly shorter than Pd−N(1) bond [2.079(4) Å]. It is also shorter than the analogous Pd−N bonds in $Na_2[Pd(SO_3)_2en]\cdot 4\,H_2O$ [2.084(2) Å].[11] Both these examples serve to emphasise the effect of the *trans*-influence of the sulfite ligands, albeit to a different extent (dependent on the total charge and coordination mode). As discussed for **1**, this is as a result of the lower *trans*-influence of the bridging oxygen atom, as compared with sulfur, on the Pd−N(2) bond in the position *trans* to it.

The influence of the ligand in the *trans*-position also affects the Pd−O bond. Here, this bond, with the less efficient nitrogen atom *trans* to it, is significantly shorter [2.043(3)

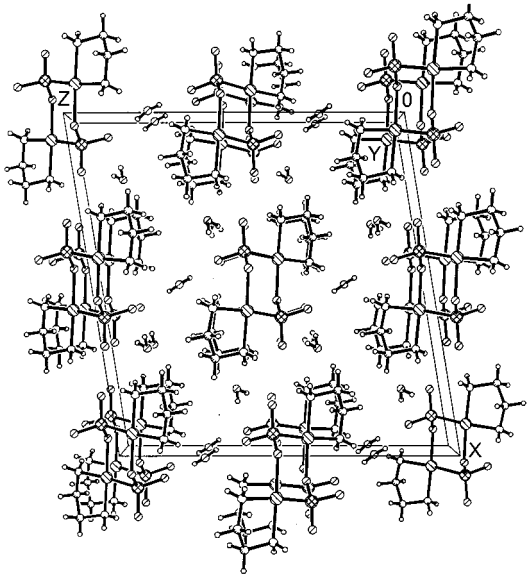

Figure 4. Molecular packing in the crystal structure of **2**

Å] than that in $K_2[Pd(SO_3)_2]\cdot H_2O$ where a sulfur atom is in the *trans*-position [2.121(3) Å].[1b]

As expected, the Pd−S bond in **2** is clearly shorter [2.229(1) Å] than that in the complex $Na_2[Pd(SO_3)_2(en)]\cdot 4\,H_2O$ [2.269(1) Å],[11] involving monodentate *S*-coordinated sulfite ligands in an anionic complex species. After the bond-valence approach,[12] weakening of one bond causes an increase of the bond orders and hence the decrease of the bond lengths in adjacent bonds. Thus, lowering of the bond order on going from almost S−O double bonds in $Na_2[Pd(SO_3)_2(en)]\cdot 4\,H_2O$ to S−O single bonds in the sulfite bridges of **2**, leads to the shortening of the Pd−S bonds. In $K_2[Pd(SO_3)_2]\cdot H_2O$, with bidentate bridging sulfite ligands, the Pd−S bonds are similarly short [2.241(1) Å].[1b]

The overall arrangement of the chair-shaped molecules in the crystal lattice of **2** is such that the hydrophilic regions of the complexes (NH_2 and SO_2 groups) approach each other. Thus, a complicated network of hydrogen bonds between these hydrophilic segments of the dinuclear complex units, and between the complexes and water molecules can be formed. Also, the intermolecular distances between the hydrophobic parts of the complexes (CH_2 groups) are short (see Figure 4).

Spectrometry

UV/Vis Spectra: The reaction between $[Pd(en)(OH_2)_2]^{2+}$ and $[Pd(SO_3)_2(en)]^{2-}$ was followed by UV/Vis spectrometry (see Figure 5). However, from the spectra it is not certain whether the dinuclear complex $[(en)Pd(SO_2O)_2Pd(en)]$ is formed first, followed by the isomerisation to $[(en)Pd(SO_2O)(OO_2S)Pd(en)]$, or whether the mononuclear complex $[(en)Pd(SO_3)(H_2O)]$ is formed (generated by the partial dissociation of the anion and recoordination of the released sulfite to the cation), which condenses prior to the crystallisation of **2**.

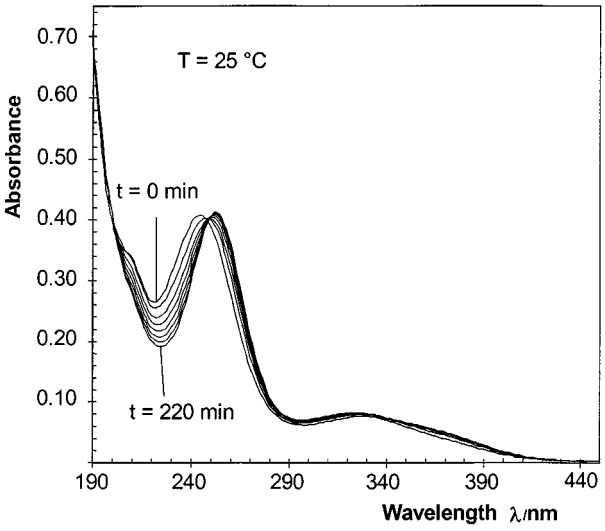

Figure 5. Time-dependent UV spectra of the reaction mixture yielding **2**

IR and Raman Spectra: The molecule of **2** (crystallographic symmetry $\bar{1}$ − C_i) has an inversion centre, in contrast to the complex unit in **1** on a general position. As a result, the mutual exclusion rule reduces the number of bands in each of the vibrational spectra of **2** to one half of that in **1**, i.e. both IR and Raman spectra of **2** are simpler. This fact is most clearly seen in the region of the valence vibrations $\nu(MN_2)$. Thus, the Raman spectrum of **1** displays four rather strong bands [two interpenetrating $\nu_s(MN_2)$/$\nu_{as}(MN_2)$ doublets] around 500 cm^{-1}, whereas the spectrum of **2** shows only two bands (see Figure 6). With respect to the differences in the Pt−N bond lengths at Pt(1) and Pt(2) (*trans*-influence), the higher doublet (574/490 cm^{-1}) is assigned to the valence vibrations of the $Pt(2)N_2$ group *trans* to oxygen and the lower one (517/442 cm^{-1}) to the $Pt(1)N_2$ fragment *trans* to sulfur. Since the angles in both PtN_2 groups are substantially smaller than 90° [81.9 and 84.2° at Pt(1) and Pt(2), respectively], the frequency sequence of their valence vibrations is always $\nu_s(PtN_2) > \nu_{as}(PtN_2)$ (cf. the reasoning in ref.[7]).

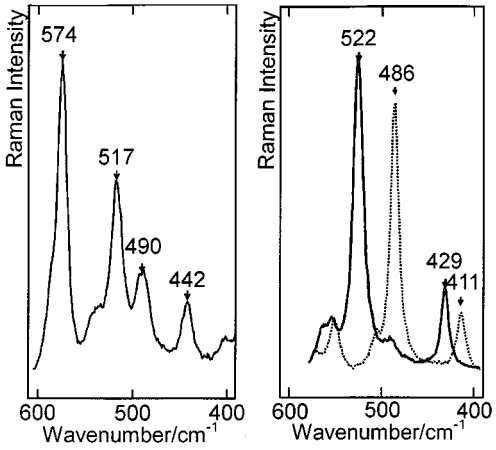

Figure 6. Raman spectra of the $\nu(MN_2)$ ranges of **1** (left), and of **2** (right) and its N-deuterated isotopomer (dotted)

In the IR spectra the result of these structural features are by far less obvious since the valence vibrations $\nu(MN_2)$ are weak. Further, these vibrations are obscured by the complex system of intense bands originating from the splitting of the deformation vibrations $\delta_{as}(SO_3)$ by the present bonding mode, with concomitant symmetry lowering, and by correlation coupling. In addition, librational modes of the three different water molecules contribute to the complexity of this spectral region. The special bonding mode also leads to three regions of valence vibrations $\nu(SO_3)$; $\nu_{as}(SO_2)$ (coarsely around 1150 cm^{-1}), $\nu_s(SO_2)$ (1050 cm^{-1}) and ν(SO) (ca. 900 cm^{-1}); for details see ref.[7] The latter vibrations are very strong in both the IR and Raman spectra of **1** and **2.** However, the bands of the SO_2 fragments are strong and broad in the IR spectra, but are of different intensity in the Raman spectra. It should be mentioned that the valence vibrations ν(CC) and ν(CN), as well as the wagging modes $\omega(NH_2)$ and $\omega(CH_2)$ of the chelate rings are expected to be in the same spectral region. Hence, a definite assignment of all the bands is difficult.

Due to the low solubilities of **1** and **2** in H_2O under ambient conditions, and its almost insoluble nature in common organic solvents, it was not possible to obtain Raman and NMR spectra of solutions.

Conclusion

On reaction of the cations $[(en)M^*(OH_2)_2]^{2+}$ and anions $[(en)M^*(SO_3)_2]^{2-}$, the expected dinuclear complex $[(en)M^*(SO_2O)_2M^*(en)]$ (in **1**) with two parallel μ-(S:O) sulfite bridges really forms in the case of M* = Pt. Thus, the repeat unit $M^*(SO_2O)_2M^*$, previously found in polymeric complexes of the type $K_2[M^*(SO_3)_2]$, is now available in an isolated stabilised form. In the case of M* = Pd, the kinetically labile starting materials probably symmetrise in two steps to form $[(en)Pd(SO_3)(OH_2)]$, prior to the condensation to the dinuclear unit $[(en)Pd(SO_2O)(OO_2S)Pd(en)]$ (in **2**) with antiparallel μ-(S:O) sulfite bridges. Seemingly, the latter is the thermodynamically controlled product, whereas in the reaction of the inert platinum(II) complexes the kinetically controlled product is formed.

These findings also raise the question of the existence of coordination polymers $^1_\infty[M^*(SO_2O)(OO_2S)]^{2-}$, with these antiparallel bridged repeat units, and also of polymers with counter-current bridges of each type, for instance $^1_\infty[M^*(SO_2O)_2M^*(OO_2S)_2]^{4-}$.

The molecular structures clearly reveal the differences of the *trans*-influence of S- and O-coordinated sulfite ligands in the same complex species. These differences and the different symmetries (non-centrosymmetric **1** vs. centrosymmetric **2**) also imprint the vibrational spectra.

Experimental Section

General Remarks: Elemental analyses for C, H, N, and S were performed using the analyser Carlo Erba Model 1108. Platinum and palladium were determined as residues after simultaneous TGA/DTA runs using the thermal analyser TA Instruments Model SDT 2960 (reference Al_2O_3).

Time-dependent UV/Vis spectra were scanned using the spectrometer HP 8452 A.

IR spectra on KBr pellets were taken with the FTIR spectrometer ATI Mattson Infinity controlled by the soft-ware package WinFirst 3.0.

Raman spectra of the pure substances in capillaries, excited with a Spectra Physics Stabilite 2014 Ar^+ laser (514.5 nm, 100 to 150 mW), were recorded using the spectrometer DILOR XY (multichannel detection) controlled by the software system XY 2.0.

X-ray structure determinations were performed with data sets collected on a four-circle diffractometer Enraf−Nonius CAD4 Mach 3, after the determination of the space groups on the basis of Weissenberg photographs. Details of the data collections for the compounds **1** and **2** are compiled in Table 4. The structures were solved with Patterson techniques and refined on F^2 using the program SHELX97.[13] In the last step of the structure refinement of **1**, the H atoms were considered with restraints for the bond lengths r(O−H), r(N−H), and r(C−H) (0.85, 0.90, and 0.96 Å, respectively), and for the bond angles in H_2O and in the H_2N groups (107 and 109°, respectively). The isotropic displacement factors of the H atoms were taken as the 1.2-fold of the equivalent U_{eq} values of the respective neighbouring atoms O, N, and C. In the case of **2** the H atoms were included in the refinement without restraints and with individual isotropic displacement factors, with the exception of the H_2O molecules (restraints 0.85 Å and 107°). − Due to the instability and the strong absorption of **1**, its structure is less accurate than that of **2**.

Crystallographic data (excluding structure factors) for the structures reported in this paper have been deposited with the Cambridge Crystallographic Data Centre as supplementary publication no. CCDC-148274 and CCDC-148275. Copies of the data can be obtained free of charge on application to CCDC, 12 Union Road, Cambridge CB2 1EZ, UK [Fax: (internat.) + 44−1223/336-033; E-mail: deposit@ccdc.cam.ac.uk].

$[(en)Pt(SO_2O)_2Pt(en)]\cdot 3\,H_2O$ (1): $[PtCl_2(en)]$ (0.326 g, 1.00 mmol) was dissolved in 10 mL of H_2O whilst heating. After cooling to about 30 °C, $AgNO_3$ (19.9 mL of a 0.1 M solution, 1.99 mmol) was added. The mixture was stirred at room temperature in the dark for at least 8 h in order for the reaction to reach completion. The precipitated AgCl was then filtered off and washed twice with 10 mL of H_2O. The combined filtrates must be completely clear and colourless. The resulting solution of $[Pt(en)(OH_2)_2]^{2+}$ was combined with a solution of $K_2[Pt(SO_3)_2(en)]\cdot 2\,H_2O$[4] (0.519 g, 0.980 mmol) in 10 mL of H_2O and kept in a refrigerator for 3 h. The reaction product deposited as a lemon-yellow, microcrystalline precipitate. To complete precipitation, 200 mL of acetone was added; the product was filtered off, washed with 20 mL of acetone, dried in an air flow, and recrystallised from 15 mL of boiling water. Yield: 0.415 g (0.587 mmol), 60.0% of the dihydrate. − $C_4H_{20}N_4O_8S_2Pt_2$: calcd. C 6.80, H 2.85, N 7.93, S 9.08, Pt 55.22; found C 7.03, H 2.77, N 7.75, S 8.82, Pt 56.4.

In order to grow single crystals, about 200 mg of the compound was dissolved in 8 to 10 mL of hot H_2O. This solution was placed in an appropriate vial and put into a well-isolated Dewar flask, so that slow cooling could take place over several days; after about a week lemon-yellow crystal platelets of the trihydrate **1**, with edge lengths of 0.2 to 1.0 mm had grown. − $C_4H_{22}N_4O_9S_2Pt_2$: calcd. C 6.63, H 3.06, N 7.73, S 8.85, Pt 53.76; found C 6.72, H 2.87, N 7.70, S 8.64, Pt 55.2.

$[(en)Pd(SO_2O)(OO_2S)Pd(en)]\cdot 3\,H_2O$ (2): $[PdCl_2(en)]$ (0.2373 g, 1.000 mmol) was dissolved in 10 mL of boiling H_2O; after cooling

Table 4. Data for crystal structure determinations of **1** and **2**; e.s.d.'s are given in parentheses

	1	**2**
Empirical formula	$C_4H_{22}N_4Pt_2O_9S_2$	$C_4H_{22}N_4Pd_2O_9S_2$
Formula mass	724.6	547.2
Crystal system	Monoclinic	Monoclinic
Space group	$P\,2_1/n$	$C\,2/c$
a [Å]	10.064(1)	17.4340(2)
b [Å]	12.486(2)	5.3276(9)
c [Å]	13.099(3)	17.016(2)
β [°]	109.52(1)	99.386(9)
Z	4	4
D_c [g·cm^{-3}]	3.102	2.330
F_{000}	1336	1080
V [Å^3]	1551.4(5)	1559.8(4)
Colour	Yellow	Yellow
Diffractometer	Enraf−Nonius CAD 4 − Mach 3 four circle	Enraf−Nonius CAD 4 − Mach 3 four circle
X-Radiation, λ [Å]	Mo-K_α, graphite monochromatic, 0.71073	Mo-K_α, graphite monochromatic, 0.71073
Crystal size [mm]	0.3×0.2×0.05	0.20×0.06×0.05
Data collect. temp. [K]	173	Ambient
Data collecting mode	ω −2θ scan	ω −2θ scan
2θ -range	5.0° ≤ 2θ ≤ 48°	5.7° ≤ 2θ ≤ 50°
$h\ k\ l$ range	−11/11, 0/14, −14/14	−20/20, 0/6, −20/20
Reflections measured	5104	3069
unique	2426	1375
observed	2130 ($I \geq 4\sigma\ (I)$]	1134 ($I \geq 4\sigma\ (I)$]
μ (Mo-K_α) [cm^{-1}]	183.3	26.2
Absorption correction	ψ -scans	ψ -scans
$T_{max}/T_{min}/T_{mean}$	99.7%/23.46%/66.67%	99.78%/73.76%/87.15%
GooF	1.050	1.051
$R(F)$ (all reflections)	0.049	0.036
$R(F)$ (observed reflections only)	0.042	0.024
$R_w(F^2)$ (all reflections)	$R_w(F^2) = 0.122$ $w = 1/[\sigma^2(F) + (A\cdot P)^2 + B\cdot P]$ $P = [\mathrm{Max}(F_0^2, 0) + 2\cdot F_c^2]/3$ $A = 0.0871$, $B = 2.52$	$R_w(F^2) = 0.057$ $w = 1/[\sigma^2(F) + (A\cdot P)^2 + B\cdot P]$ $P = [\mathrm{Max}(F_0^2, 0) + 2\cdot F_c^2]/3$ $A = 0.0241$, $B = 0.00$

to about 30 °C, $AgClO_4$ (0.413 g, 1.99 mmol) in 20 mL of H_2O was added. After stirring at room temperature in the dark for 4 h, AgCl that had precipitated was filtered off and washed twice with 10 mL of H_2O. The clear and colourless solution of $[Pd(en)(OH_2)_2](ClO_4)_2$ was cooled with ice and mixed with $K_2[Pd(SO_3)_2(en)]\cdot 2\,H_2O$[4] (0.432 g, 0.980 mmol) in 10 mL of H_2O (0 °C); the reaction mixture turned lemon-yellow within a few seconds. After stirring for 10 s, the precipitated $KClO_4$ was filtered off and washed twice with 5 mL of cold H_2O. The combined yellow filtrate was poured into 200 mL of cooled acetone, the formed yellow precipitate was filtered off, washed with a few mL of cold acetone, dried for a short time in air, and finally over P_4O_{10} in a desiccator under ambient pressure. This procedure yielded 0.346 g (0.654 mmol), 65.4% of a dihydrate. − $C_4H_{20}N_4O_8S_2Pd_2$: calcd. C 9.08, H 3.81, N 10.59, S 12.12, Pd 40.22; found C 9.16, H 3.87, N 10.5, S 12.2, Pd 41.9.

On diffusion of acetone vapour into a solution of 0.100 g of the dihydrate in 5 mL of H_2O, at ambient temperature in the dark, yellow prismatic crystals of the trihydrate **2** grew on the glass walls within some days. − $C_4H_{22}N_4O_9S_2Pd_2$: calcd. C 8.78, H 4.05, N 10.24, S 11.72, Pd 38.90; found C 8.91, H 3.90, N 10.0, S 11.3, Pd 37.6.

Acknowledgments

The authors thank the Verband der Chemischen Industrie − Fonds der Chemischen Industrie, Frankfurt/Main, and the Universitätsbund Erlangen-Nürnberg for financial support, and DEGUSSA, Hanau, for gifts of the platinum-group metals.

[1] [1a] W. Haegler, Thesis, University of Erlangen-Nürnberg, **1979**. − [1b] D. Messer, D. K. Breitinger, W. Haegler, *Acta Crystallogr., Sect. B* **1979**, *35*, 815.
[2] G. Bauer, Thesis, University of Erlangen-Nürnberg, **1979**.
[3] B. Ballet, A. Bino, S. Cohen, H. Rubin, T. Zor, *Inorg. Chim. Acta* **1991**, *188*, 91.
[4] R. Krieglstein, Thesis, University of Erlangen-Nürnberg, **1997**.
[5] R. Eskenazi, J. Raskovan, R. Levitus, *J. Inorg. Nucl. Chem.* **1965**, *27*, 371.
[6] M. Raidel, Thesis, University of Erlangen-Nürnberg, **1985**.
[7] R. Krieglstein, D. K. Breitinger, *J. Mol. Struct.* **1997**, *408/409*, 379.
[8] D. H. Farrar, R. R. Gukathasan, *J. Chem. Soc., Dalton Trans.* **1989**, 557.
[9] F. A. Cotton, G. Wilkinson, *Advanced Inorganic Chemistry*, 5th Ed., John Wiley & Sons, New York − Chichester − Brisbane − Toronto − Singapore, **1988**, p. 1094.
[10] B. Lippert, C. J. L. Lock, B. Rosenberg, M. Zvagulis, *Inorg. Chem.* **1978**, *17*, 2971.
[11] D. K. Breitinger, G. Schottner, M. Raidel, H. P. Beck, *Z. Anorg. Allg. Chem.* **1986**, *539*, 18.
[12] I. D. Brown, D. Altermatt, *Acta Crystallogr., Sect. B* **1985**, *41*, 244.
[13] G. S. Sheldrick, *SHELX97*, *Program for Crystal Structure Refinement*, University of Göttingen, Germany, **1997**.

Received December 14, 2000
[O00473]